Journal of Thermal Engineering
Web page info: https://jten.yildiz.edu.tr
DOI: 10.14744/thermal.0000000

Research Article

Experimental adsorption studies of atmospheric water vapor by clay based composite sorbents in vertical fluidized bed

C. R. HIREMATH[1,*], Ravikiran KADOLI[2], R. J. TALAPATI[3]

[1]Department of Mechanical Engineering, BLDEA's V. P. Dr. P. G. Halakatti College of Engineering and Technology, Vijayapur-Karnataka, 586103, India
[2]Department of Mechanical Engineering, National Institute of Technology Karnataka, Surathkal, 575025, India
[3]Department of Mechanical Engineering, KLS Vishwanathrao Deshpande Institute of Technology, Haliyal, 581329, India

ARTICLE INFO

Article history
Received: 21 August 2024
Revised: 14 December 2024
Accepted: 18 December 2024

Keywords:
Adsorption; Clay; Calcium chloride; Fluidization; Horse dung; Humidity ratio; Sawdust

ABSTRACT

Transient adsorption characteristics of atmospheric water vapor with clay and clay-additives-based calcium chloride composite desiccants in vertical fluidized beds are studied experimentally. The different clay-based composite sorbents considered in the study are clay-calcium chloride, clay-horse dung-calcium chloride and clay-sawdust-calcium chloride adsorbents. The influence of bed mass and air superficial velocity on transient change in bed inlet air humidity ratio and air temperature for different desiccant clay-based composite sorbents is experimentally studied. It was noted that the thermo-physical properties of different adsorbents, bed mass and air inlet velocity significantly influence the fluidized bed performance in the adsorption system. The linear porosity distribution in fluidization shows the availability of increased adsorption capacity for clay-based desiccants in comparison to clay-additive desiccants, as indicated by higher total adsorption capacity. For the similar conditions of bed weight (300 g) and inlet air velocity (2 m/s), the total quantity of water adsorbed is 30.09 g, 21.84 g and 27.02 g for clay-calcium chloride, clay-horse dung-calcium chloride and clay-sawdust- calcium chloride fluidized adsorbent beds. The results reveal heat load reduction of clay-calcium chloride vertical fluidized bed dehumidification system is 62% and 52% higher compared to clay-horse dung-calcium chloride and clay-sawdust-calcium chloride desiccant dehumidification systems. For all the dehumidification systems, the reduction in latent load is higher than the increase in sensible heat load, which will reduce the overall heat load of the cooling system.

Cite this article as: Hiremath CR, Kadoli R, Talapati RJ. Experimental adsorption studies of atmospheric water vapor by clay based composite sorbents in vertical fluidized bed. J Ther Eng 2025;11(5):1−18.

***Corresponding author.**
*E-mail address: chandra.hiremath@yahoo.com

This paper was recommended for publication in revised form Editor-in-Chief Ahmet Selim Dalkilic.

INTRODUCTION

The demand for economical, environmentally friendly, energy-efficient air conditioning and refrigeration systems is increasing daily. Using refrigerants in traditional air conditioning and refrigeration systems, such as hydro chlorofluorocarbons and chlorofluorocarbons, endangers the ozone layer and contributes to global warming. Because of this, sorption-based air conditioning systems are becoming more and more critical. In desiccant cooling, the air is dehumidified and then sensibly cooled before being supplied to the conditioned space, a relatively newer air conditioning technique. The capability of the adsorbent material to adsorb water vapor is a critical factor in dehumidification performance. The desiccant-based system is used in applications such as heating, ventilation, air conditioning and refrigeration (HVACR) system, energy and environment, drying of grains and cereals, food preservation, freshwater production, filtration, purification processes, dehumidification, pollution control, wastewater treatment and thermal energy storage system [1-7]. The parameters influencing the desiccant-based system's effectiveness are desiccant bed configuration and desiccant material properties. The conventional packed bed system is commonly employed in sorption-based systems, and it has been noted that flow through the packed bed is not entirely uniform. At any instant in time, the adsorbents above or below the mass transfer zone do not participate in the mass transfer process. Lv bo et al. [8] investigated liquid-solid fluidized bed's fluidization properties and adsorption efficiency using batch, cyclic and continuous adsorption characteristics. The fluidized bed layer's external diffusion rate increased due to high-frequency contact between adsorbent and adsorbate. The results showed that a fluidized bed is more effective than a packed bed in adsorption. Krzywanski et al. [9] investigated the fluidized bed-to-surface heat transfer and fixed beds of adsorption chillers. Compared to a conventional packed bed, a fluidized bed of adsorbents showed a considerable increase in bed-to-wall heat transfer coefficient. Further, it was revealed that the proposed concept of a fluidized bed will reduce the chiller's size, eliminating the fundamental barrier to broader adoption of adsorption cooling technology.

Hamed [10] experimentally investigated the desorption and adsorption behavior of an inclined fluidized bed with silica gel as a desiccant. It was observed that the adsorption rate was highly affected by inlet air velocity. Horibe et al. [11] experimentally investigated sodium polyacrylate sorbent's fluidized bed sorption behavior with multiple cooling pipes. It was revealed that numerous cooling pipes resulted in a more excellent sorption ratio and a shorter sorption process completion time. Ye et al. [12] developed soybean seeds' contact sorption-fluidized bed drying system from the perspective of energy efficiency and product quality. The drying rate was improved with gas velocity and mass ratio of silica gel. Experimental results showed an improvement in the quality of dried seeds since drying is carried out in a consistent environment of low humidity. Sobrino et al. [13] experimentally studied the effect of rotational distributor plates on vertical cylindrical bed behavior. The proposed bed design promotes the radial distribution of particles, reducing high-concentration zones and preventing temperature gradients like hot spots in a fluidized bed. Hamed et al. [14] studied the transient adsorption/desorption behavior of spherical particles of silica gel in a fluidized bed. The maximum decrease in air humidity was reported at the beginning of adsorption. Wang et al. [15] conducted an experimental study on the performance of fluidized bed adsorber/desorber containing a working pair of adsorption refrigeration systems with activated carbon. The experiments were performed for different masses of activated carbon, and enhancements were observed for 2 Kg and 3 Kg of activated carbon adsorbent. However, the effectiveness of 4 Kg adsorbent in fluidized adsorber and desorber was low due to incomplete fluidization of activated carbon. Horibe et al. [16] experimentally investigated sorption desorption characteristics of organic sorbent HU720PR in two-chamber connected fluidized beds. It was reported that dehumidification performance was highly influenced by the initial bed height of the sorbent and the temperature difference between sorption and desorption chambers. Zettl et al. [17] developed a rotating drum filled with zeolite to avoid the non-reactive zones. Due to the moving reaction bed, the whole volume will contribute to adsorption dehumidification in distinction to fixed bed vessels. Li et al. [18] proposed a novel compact micro fluidized bed (CMFB) to remove carbon dioxide from indoor air using resin-based polyethyleneimine solid adsorbent in HVAC. CMFB's saturation adsorption time was 17% shorter than a fluidized bed (FB). A fluidized bed provides a means for achieving intimate gas-sorbent contacting and mixing. The results showed that a fluidized bed is more effective than a packed bed in the adsorption process. Fluidization might be very useful in increasing the adsorption-desorption characteristics of sorbents in a desiccant column.

Studies on chemical desiccants and their composites have been studied in packed and fluidized bed configurations. Still, only few studies have been published on biomass-based and environmentally friendly natural desiccants [19]. Impregnation of sodium chloride deliquescent salt within a super-porous hydrogel polymer matrix improved desiccant performance threefold [20]. The driving force behind this improved performance is the porous structure of the polymer matrix. The potential use of natural materials and their composites as desiccants for water vapor extraction and evaporative cooling was investigated.

Kumar et al. [21] investigated saw wood-calcium chloride composite desiccant on water production from atmospheric air. Freshwater production from ambient air depends on the amount of calcium chloride. Hiremath et al. [22] investigated clay's transient heat and mass transfer behavior as the desiccant carrier with sawdust and horse

dung as additives. Liang et al. [23] reported the effect of geometrical factors on an improved circulating inclined fluidized bed for an HVAC duct system. The optimal ICIFB arrangement resulted in minimum pressure drop and high energy factor compared to circulating erect fluidized bed (CEFB). Thus, an optimal ICIFB system was beneficial for lowering energy consumption. Timsina et al. [24] reported the influence of different particle sizes on fluidization characteristics. Compared to the experiment with only large particles, the lowest fluidization velocity with 20% tiny and 80% large particles was reduced by 60.8%.

Singh et al. [25] investigated moisture desorption and sorption behavior of cocopeat, sawdust and dried cow dung in the evaporative cooling system. Experimental results showed that dried cow dung and coco-peat had the potential to replace chemical desiccants. Dorothea and Dimitrios [26] explored the application of spruce sawdust processed with sulfuric acid and diethylene glycol to remove hexavalent chromium from wastewater. The rate of adsorption capacity was found to increase by 84% for sawdust pretreated with 50% diethylene glycol and by 89% for sawdust pretreated with sulphuric acid. Dasar et al. [27] investigated dried cow dung's sorption and desorption behavior with Polyvinyl Pyrrolidone and clay as a binder. It was reported that dried cow dung with Polyvinyl Pyrrolidone could replace chemical desiccants due to its exergy efficiency and moisture absorption capability. One of the benefits of a fluidized bed system over a packed bed system is the high heat and mass transfer rate among gas and particles, as reported in the literature study.

Previous studies were published using commercially available silica gel in fluidized bed configurations and their sorption performances. A few studies on clay and clay-based sorbents in fluidized beds were discussed. Besides desiccant and bed configurations, literature on using calcium chloride as the desiccant and biomaterial is minimal [28]. To fill this research gap, the current study explores the effect of clay, clay-based sorbents in dehumidifying the atmospheric air using vertical fluidized bed arrangement.

Most of the earlier research was done on chemical desiccants and their mixtures. Although there are few studies on using natural desiccants in the open literature, dried cow dung has a very promising moisture uptake capacity; however, during the desorption process, the binding strength is lost, resulting in a mass reduction of the desiccant. Using clay and clay-additive desiccants in vertically packed beds releases heat of adsorption, increasing the bed exit air temperature and bringing an additional heat load [29]. The increase in outlet air again becomes a source of energy consumption that requirements to be resolved. For this reason, sorbent-based fluidized beds with high heat and mass transfer rates are promising alternatives suitable for air-conditioning systems. The fluidized bed system has a lot of benefits regarding the energy savings of an air-conditioning system with effective dehumidification performance diminishing the scale of the system, low extra-sensible heat load reducing the system load [30]. The research aims to study the adsorption characteristics of atmospheric water vapor with desiccants based on clay in a vertical fluidized bed (VFB). Naturally available clay and hygroscopic inorganic salts are employed to prepare sorbents. Low-cost biomaterials like horse dung and sawdust are utilized as additives. The experimental study was conducted to understand the influence of bed mass and air inlet velocity on transient change in bed air humidity ratio and air temperature for different desiccant clay-based composite sorbents. The different clay-based composite sorbents considered in the study are clay-calcium chloride, clay-horse dung-calcium chloride and clay-sawdust-calcium chloride adsorbents. Furthermore, heat load calculations and exergy analyses are performed to measure the capabilities of these novel desiccant composites.

DESICCANT MATERIALS AND EXPERIMENTAL SYSTEM

Desiccant Materials

In the present study, composite desiccants made of clay are employed. The desiccants are prepared from naturally available clay, biomaterials like horse dung and sawdust as additives and commercially available hygroscopic calcium chloride inorganic compound. The clay is procured from a local pot maker, which prepares baked pots and oil lamp fixtures. Horse dung, popularly employed by local pot makers to prepare porous pots, is selected as an additive. Sawdust, a sawmill residue, is another additive with horse dung. The cleaned clay and segregated additives are combined in the proportion of 1:20 by mass. The mixture of clay and additives is thoroughly wetted by water, and separate pasty material of clay, clay-horse dung and clay-sawdust are obtained. The ready pasty material is then extruded through a syringe. The syringe has a needle of 2 mm diameter. The extrusion process produces an extended cylindrical-shaped structure of 2 mm diameter. The overlong cylinder is then cut to a length of 2 mm along its length. Thus, cylindrical-shaped desiccants of size 2 mm × 2 mm are prepared. clay lumps and desiccants based on clay additions are heat treated to 500°C in a muffle furnace. The heat treatment removes the initial desiccant moisture and induces strength and rigidity. The photographs of prepared desiccants before saturation with calcium chloride hygroscopic solution are shown in Figure 1.

A calcium chloride solution with a concentration of 50% is prepared by dissolving granules of calcium chloride in distilled water. To avoid catching atmospheric moisture, the solution is kept in an airtight jar. The calcium chloride desiccant solution is prepared by impregnating lumps of heat-treated clay and clay-additive desiccants. The duration of impregnation is 24 hours. Following that, soaked particles are filtered and later dried in the furnace. Further, to ensure the impregnation and depth of penetration of calcium chloride into the pores of desiccants, scanning electron microscopy

(a) (b) (c)

Figure 1. Photographs of heat treated (a) clay (b) clay-horse dung and (c) clay-sawdust desiccants.

(SEM) image analysis is carried out. The images of the halved portion of clay-calcium chloride, clay-horse dung-calcium chloride and clay-sawdust-calcium chloride at 2000-X magnification are shown in Figure 2.

The surface examination of images reveals a porous nature with interconnected voids and valleys. Further, it shows a smoother surface (see Figure 2(a) and 2(b)) appearance for clay additives composites as a rough surface for clay without additives (see Figure 2(c)). The white flaky and spongy appearance qualitatively ensures the depth and penetration of calcium chloride onto the surface. The surface pattern of clay-calcium chloride shows the existence of inter-particle macro-pores, whereas clay-horse dung-calcium chloride and clay-sawdust-calcium chloride indicate dispersed micro-pores

The thermo-physical properties of prepared desiccants are shown in Table 1 [22, 31]. The higher porosity and water content decrease the thermal conductivity of clay-horse dung-calcium chloride and clay-sawdust-calcium chloride by 16.75 % and 29.56% pertaining to the clay-calcium chloride desiccant. Maximum thermal diffusivity values are being reported for clay-based composite desiccants. Lower porosity in clay-calcium chloride desiccants signifies higher density than clay-additives-based desiccants. The higher water content in clay-additives-based desiccants contributes to higher specific heat capacities.

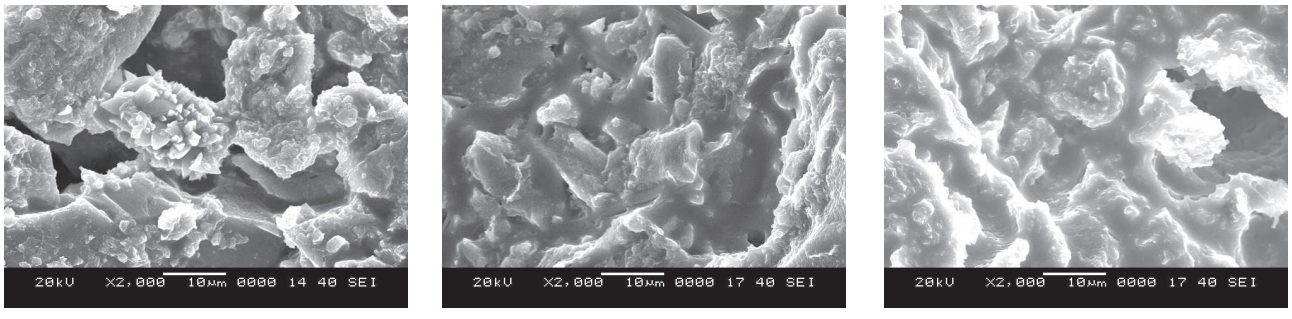

(a) **(b)** **(c)**

Figure 2. Scanning electron microscope images of clay composite desiccants showing cut-sections (a) clay-calcium chloride (b) clay-horse dung- calcium chloride (c) clay-sawdust-calcium chloride.

Table 1. Properties of different solid composite adsorbent

Adsorbent	Thermal diffusivity (m^2/s)	Specific heat (J/kg K)	Thermal conductivity (W/m^2 K)	Density (Kg/m^3)	Porosity (%)	Initial water content (g water/kg adsorbent)
Clay- calcium chloride	6.54×10^{-5}	832.5	2.03	2372	13	63.79
Clay-horse dung- calcium chloride	4.54×10^{-5}	1392	1.69	1456	26	94.44
Clay-sawdust-calcium chloride	3.30×10^{-5}	1461	1.43	1114	23	86.03

Experimental Methodology

The present experimental setup is the same as reported in Hiremath et al. [22] and is used to conduct dehumidification experiments. The components of the experimental arrangement are an interconnected air compressor, air heating unit and vertical desiccant column, shown in Figure 3. The system is a single-blow, open-loop adsorption experiment. Air from the compressor is directed through a galvanized iron pipe of 25 mm diameter to the vertical bed column. Flow control valves (V1, V2) regulate the process airflow direction for adsorption experiments. To visualize the fluidized bed behavior, the vertical cylindrical desiccant test section is constructed with transparent acrylic material. The schematic diagram and photograph image of various phases of fluidization are shown in Figure 4 and Figure 5. The size of a single cylindrical adsorbent and regeneration bed is 700 mm in height, 50 mm in diameter and 4 mm thick. A flange connects the vertical bed and the experiment's primary pressure line with the nut and bolts system. For uniform distribution of air stream, a fine wire mesh of stainless steel is fixed at the lower part of a bed. The bed's bottom and flange are properly sealed to prevent the leakage of desiccants and air stream. The vertical bed height (700 mm) is sufficient to prevent the loss of desiccants from the upper part of the bed, as the maximum fluidization height attained during experimentation is 650 mm. The vertical column has taps for placing the hygro-transmitter at the inlet and outflow of the vertical bed column and pressure taps. During the initial stages of fluidization, the air moves through the bed, gets loosened, and dense phase fluidization occurs. The clay composite desiccant moves away from each other, creating voids for the passage of air. This indicates the desiccant bed begins to experience smooth fluidization (see Figure 5(a)). The voids created due to the separation of the desiccant provide passage for airflow because air flows at fluidization velocity, and the desiccant is further taken into a state of buoyancy. This increased the bed height, and the fluidization type switched to bubbling fluidization (see Figure 5(b)).

Once the desiccants start to bubble, the momentum of air is such that the desiccant is carried along with the air stream, achieving complete fluidization. The bed behavior changes from bubbling fluidization to a turbulent fluidization regime (see Figure 5(c)). All desiccants are well circulated, the bed reaches the maximum height and all desiccants are entrained into the vertical bed.

The minimum superficial velocity (v) to overcome gravitational energy required for fluidization should be known and is estimated from the Leva equation [32]. The minimum value of fluidization velocity estimated using Leva equation for clay-calcium chloride and clay - additives - calcium chloride desiccants is checked and validated during experiments.

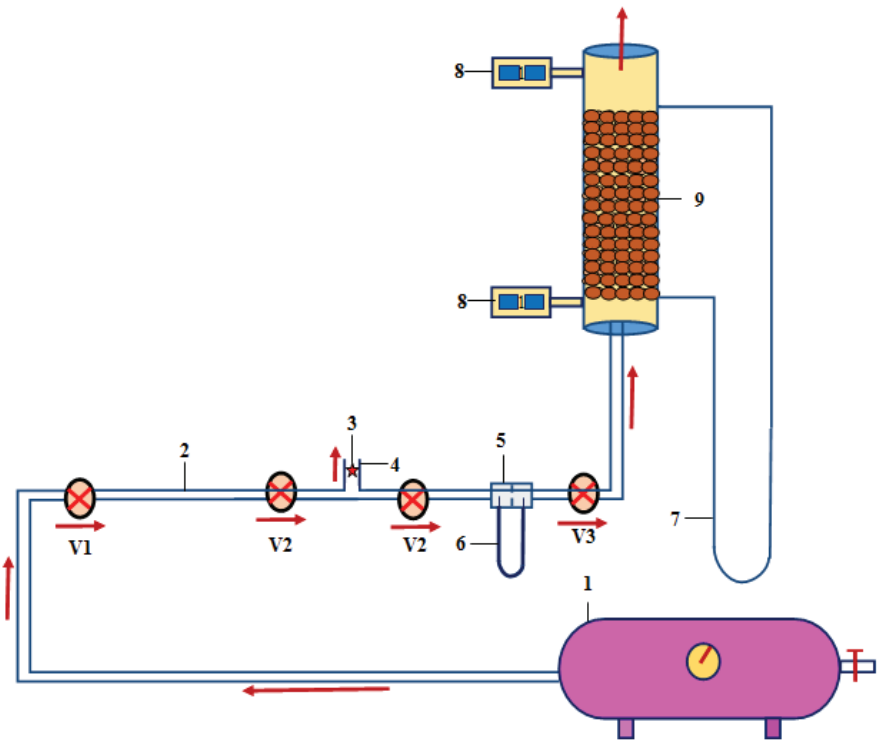

1. Air compressor 2. Pressure line 3. Thermocouple 4. Pressure line vent 5. Orifice meter 6, 7. U-Tube manometer 8. Hygrometer 9. Fluidized bed. 10. Control valves (V1, V2, V3, V4).

Figure 3. Experimental set up layout.

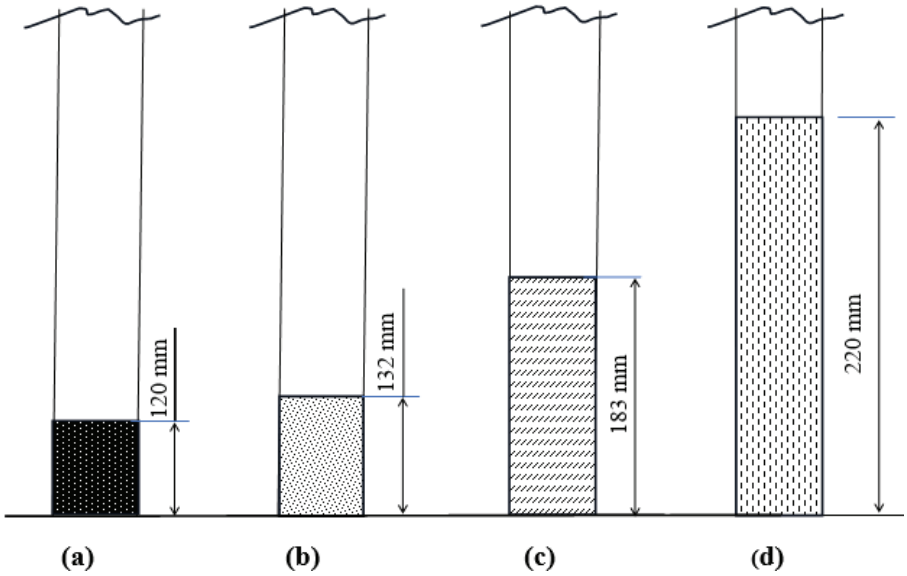

Figure 4. Schematic diagram of various phases of fluidization of clay - horse dung - calcium chloride for m=200 g, v=1.5 m/s. (a) Packed bed (b) Dense phase fluidization (c) Bubbling fluidization (d) Turbulent fluidization.

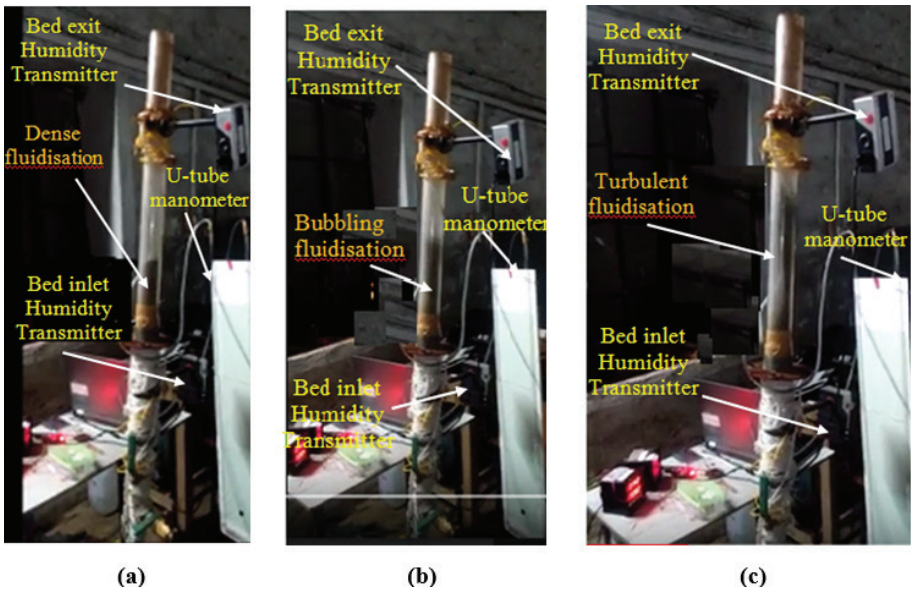

Figure 5. Photograph showing regimes of fluidization (a) Dense fluidization (b) Bubbling fluidization and (c) Turbulent fluidization.

Table 2. Validation of minimum fluidization velocity

Desiccant bed	Bed weight (g)	Minimum fluidization velocity (Experimental, m/s)	Minimum fluidization velocity (Theoretical, m/s)
Clay-calcium chloride	200	1.26	1.87
Clay - sawdust-calcium chloride	200	1.70	1.20
Clay - horse dung-calcium chloride	200	1.74	1.18

Before the fluidization experiments the minimum fluidization velocity for bed weight 200 g was measured and is shown in Table 2. The experimentally tested minimum fluidization velocity for bed mass of 200 g bed weight is about 1.26 m/s to 1.74 m/s. The theoretically estimated velocity for clay-calcium chloride and clay-additives-calcium chloride desiccant ranges from 1.20 m/s to 1.87 m/s.

Data reduction

The actual volume flow rate of air through orifice flow meter is given by following equation: [33];

$$Q_{act}=\frac{C_d A_1 A_2 \left(2gh\right)^{0.5}}{\left(\left(A_1\right)^2-\left(A_2\right)^2\right)^{0.5}} \tag{1}$$

The density of process air is obtained from ideal gas relation by using equation (2) [33];

$$\rho_a=\frac{P_a}{R_a T_a} \tag{2}$$

Equation (3) calculates the mass flow rate of air [33];

$$\dot{m}=\rho_a \times Q_{act} \tag{3}$$

The process air superficial velocity at bed inlet is estimated by equation (4) [33];

$$v_a=\frac{\dot{m}}{\left(\rho_a \times \frac{\pi}{4} d_b{}^2\right)} \tag{4}$$

The vapor pressure (P_w) at desiccant bed entry and exit as a function of relative humidity (ϕ) and saturation pressure (P_{sat}) is given by equation (6). The saturation pressure at bed inlet and exit as a function of temperature of air is given by equation (5) [34];

$$P_{sat}=610.78\times e^{\frac{(17.2694\times T_a)}{(T_a+273)}} \tag{5}$$

$$P_w=\phi \times P_{sat} \tag{6}$$

The humidity ratio (H_R) of process air at bed inlet and exit is given by equation (7) [34];

$$H_R=\frac{0.622\times P_w}{P_{total}-0.378\times P_w} \tag{7}$$

The linear variation of bed porosity (ε_z) along the bed length in fluidization is given by equation (8) [34];

$$\varepsilon_{b_z}=\left(\varepsilon_{\min}\right)+\left(\frac{z}{L}\right)\left(\varepsilon_{\max}-\varepsilon_{\min}\right) \tag{8}$$

The total adsorption rate ($M_{sat}(t)$) is the amount of water adsorbed during a specific period and is obtained by taking integral of transient adsorption rate with process time as given by equation (9) [35];

$$M_{ads}(t)=\dot{m}\int_0^t \left(H_{R_i}(t)-H_{R_e}(t)\right)\Delta t \tag{9}$$

Adsorption heat released during moisture uptake increases the temperature of air. This heat is undesirable in evaporative cooling but can be indirectly cooled to condition the room. The total heat load includes both sensible and latent heat load. The decrease in sensible heat load for unit mass flow rate due to decrease in temperature of the air can be estimated by equation (10) [27];

$$Q_S=C_{p_a}(T_i-T_e) \tag{10}$$

The decrease in latent heat load because of a reduction in moisture content from the air. Latent heat load for unit mass flow rate is given by equation (11) [27];

$$Q_L=h_{fg_v}(H_{R_i}-H_{R_e}) \tag{11}$$

The sensible heat factor (SHF) is given by equation (12) [27];

$$SHF=\frac{Q_S}{(Q_S+Q_L)} \tag{12}$$

Exergy of process air comprises thermal exergy and chemical exergy. The change in thermal exergy is due to heat and mass transfer between desiccant and the process air. The change in chemical exergy is due to variation in mass of Calcium chloride contained in the pores of desiccant. The exergy of process air at the desiccant bed inlet is given by equation (13) [36];

$$\begin{aligned}E_{X_i}=&\left(C_{p_a}\right)+\left(H_{R_i}C_{p_v}\right)T_o\left[\frac{T_i}{T_o}-1-\ln\frac{T_i}{T_o}\right]\\&+R_o T_o\left[1+1.608H_{R_i}\ln\frac{(1+1.608H_{R_o})}{(1+1.608H_{R_i})}+1.608H_{R_i}\ln\frac{H_{R_i}}{H_{R_o}}\right]\end{aligned} \tag{13}$$

The exergy of process air at the desiccant bed outlet is given by equation (14) [36];

$$\begin{aligned}E_{X_e}=&\left(C_{p_a}\right)+\left(H_{R_e}C_{p_v}\right)T_o\left[\frac{T_e}{T_o}-1-\ln\frac{T_e}{T_o}\right]\\&+R_o T_o\left[1+1.608H_{R_e}\ln\frac{(1+1.608H_{R_o})}{(1+1.608H_{R_e})}+1.608H_{R_e}\ln\frac{H_{R_e}}{H_{R_o}}\right]\end{aligned} \tag{14}$$

The exergy destruction (E_Y) in water vapor adsorption is given by equation (15) [36];

$$E_Y=E_{X_i}-E_{X_e} \tag{15}$$

The exergy efficiency of desiccant dehumidifier is given by equation (16) [36];

$$\eta = \left[\frac{E_{X_i} - E_Y}{E_{X_i}} \right] \quad (16)$$

Measurements and Instrument Uncertainty

The experimental setup shown in Figure 3 is equipped with the following instrumentation to measure the parameters in adsorption experiments:

- Two Hygroflex hydro transmitters are fixed at the inlet and outlet of the vertical bed column to measure unsteady values of relative humidity and air temperature with an accuracy of ± 1% RH for 0 % to 100 % relative humidity and ± 0.2 °C for temperatures range of -40°C to 85 °C.
- Pressure drops across the orifice meter, and the vertical fluidized bed is obtained using two water-filled U-Tube manometers. The accuracy of the manometers is 1 mm.
- The volume flow rate of air is estimated with an orifice flow meter of 10.12 mm diameter, and the coefficient of discharge (C_d) is 0.68.
- The mass is measured using a digital balance with a range of 0. of 2 g to 300 g with a resolution of 0.01 g.
- The air temperature in the pressure line is measured using a calibrated K-type thermocouple (Chromel - Alumel) having a temperature range of -5 °C to 1260 °C.

The uncertainty value for the dependent parameter humidity ratio (H_R) is uncertainty in the measurement and calculation of saturation pressure (P_{sat}), vapor pressure (P_w) and relative humidity (ϕ). The superficial velocity (v_a) is a function of manometer deflection (x). Therefore, uncertainty analysis is carried out to evaluate the error or deviation in calculated parameters by the error propagation [37, 38]. Substituting measured and calculated data in equations (17) and (18) calculates the uncertainty in the experimental parameters like humidity ratio and superficial velocity.

$$\pm \sqrt{\left(\frac{\partial H_R}{\partial P_w}\right)^2 \times \left(\left(\left(\frac{\partial P_w}{\partial \phi}\right)^2 \times (\omega\phi)^2 \right) + \left(\left(\frac{\partial P_w}{\partial P_{sat}}\right)^2 \times (\omega P_{sat})^2 \right) \right)} \quad (17)$$

Table 3. Uncertainties in the measurement of experimental parameters

Parameter	Uncertainty (%)	
	m = 200 g	m = 200 g
Saturation pressure (P_{sat})	±0.64	±0.92
Vapor pressure (P_v)	±0.78	±1.36
Humidity ratio (H_R)	±0.78	±1.39
Superficial velocity (v_a)	±0.24 %	±0.40 %
Mass of bed (m)	±0.005%	±0.003%
Temperature of air (T_a)	±1	±1

$$\pm \sqrt{\left(\frac{\partial v}{\partial x}\right)^2 \times (\omega x)^2} \quad (18)$$

The parameters of the bed's weight (m) and the air's temperature (T_a) are measured directly with calibrated devices. The maximum values of uncertainty of the physical parameters, which cannot be measured directly, and the parameters that are measured directly in the experimental runs are presented in Table 3.

RESULTS AND DISCUSSION

Adsorption Performance of Clay and Clay Based Calcium Chloride Composite Adsorbents in a Vertical Fluidized Bed

The transient variation of fluidized bed air humidity ratio, air temperature at inlet and exit conditions for different air velocities, and bed mass are shown in Figures 6 - 7. For every adsorption experimental result, the humidity ratio trends and exit air temperature are similar. Maximum reductions in humidity and temperature of bed exit air relative to inlet air temperature are seen during the first phase of fluidization. The decrease in humidity results from higher initial dryness of the bed. Apart from dryness, lower vapor pressure on the desiccant surface and the higher interfacial area between the desiccant surface and surrounding air lowers the humidity of air leaving the bed [39]. The adsorption rate is higher in the early stages of the dehumidification process and gradually decreases over time. When the process starts first, the vapor pressure on the bed's surface is lower than the vapor pressure in the air. The wall portions in pores provide a mass transfer area. The distances over which moisture travels are decreased by the increase in mass transfer area between process air and desiccants owing to fluidization. The pores are filled with water vapor with time, decreasing the effective interfacial area available for mass transfer. Filling the pores with vapor decreases the calcium chloride concentration, increasing the vapor pressure on the desiccant's surface and directly affecting the potential mass transfer from air to bed. The change in calcium chloride concentration affects the potential mass transfer from the start of the experiment to the end state [39]. The transient change of the bed's exit air humidity and air temperature of 200 g and 300 g clay-calcium chloride desiccants at the bed's air inlet velocity for 1.5 m/s, 2 m/s is shown in Figure 6(a) - 6(b) and Figure 7(a)-7(b). The maximum reduction in humidity ratio for 200 g clay-calcium chloride bed mass exposed to the bed's air inlet velocity of 1.5 m/s and humidity of 5.65 g/kg is 44.04% (see Figure 6(a)). In contrast to the bed's entrance air temperature of 28.86°C, the average temperature of the bed's exit air is 27.24°C (see Figure 7(a)). With a bed mass of 300 g and an air velocity of 2 m/s, the maximum reduction in humidity is around 43.74% (see Figure 6(b)), and exit air attains a maximum temperature of 27.84°C relative to an inlet air temperature

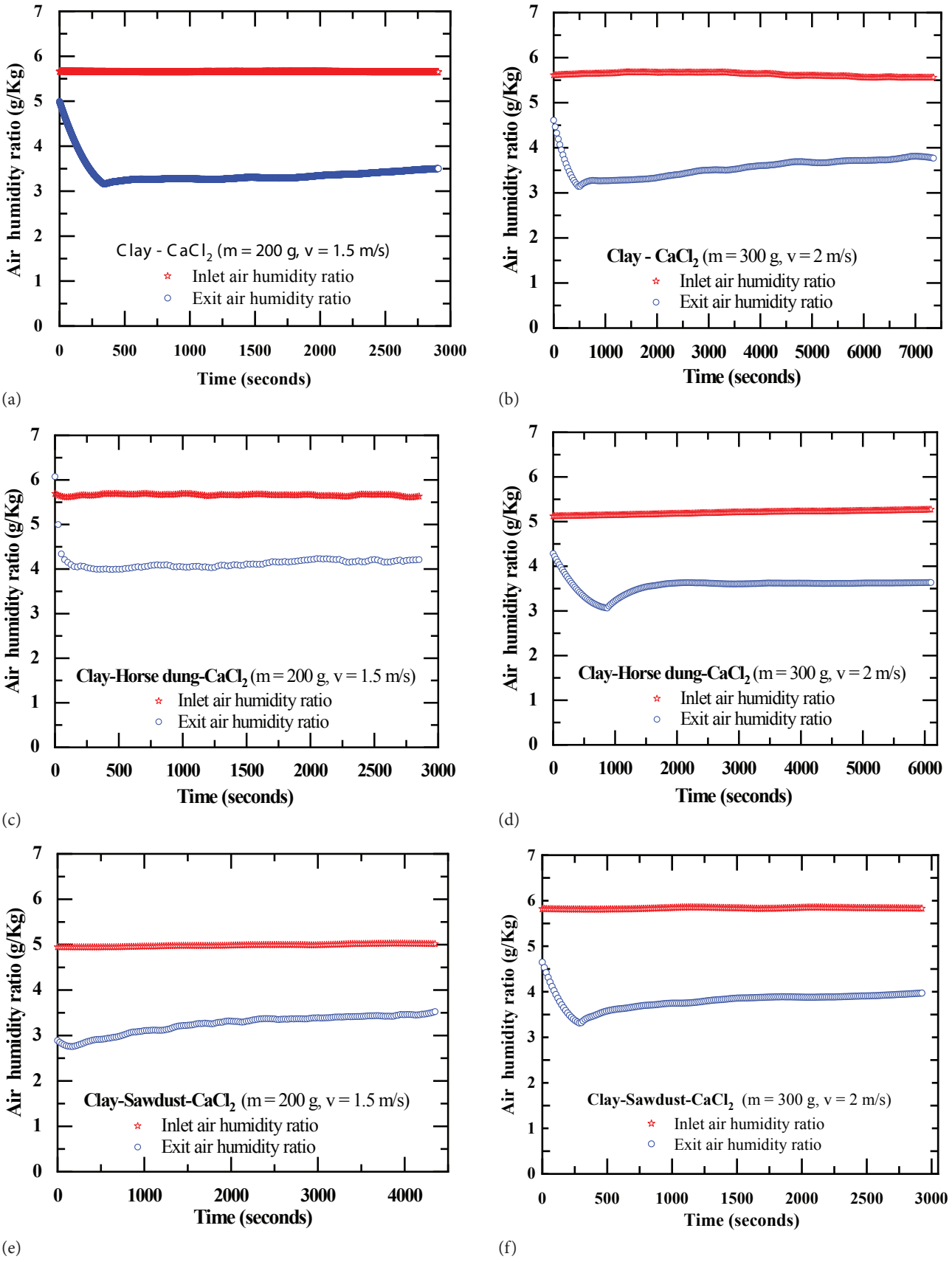

Figure 6. Air humidity ratio characteristics of different desiccants for adsorption process.

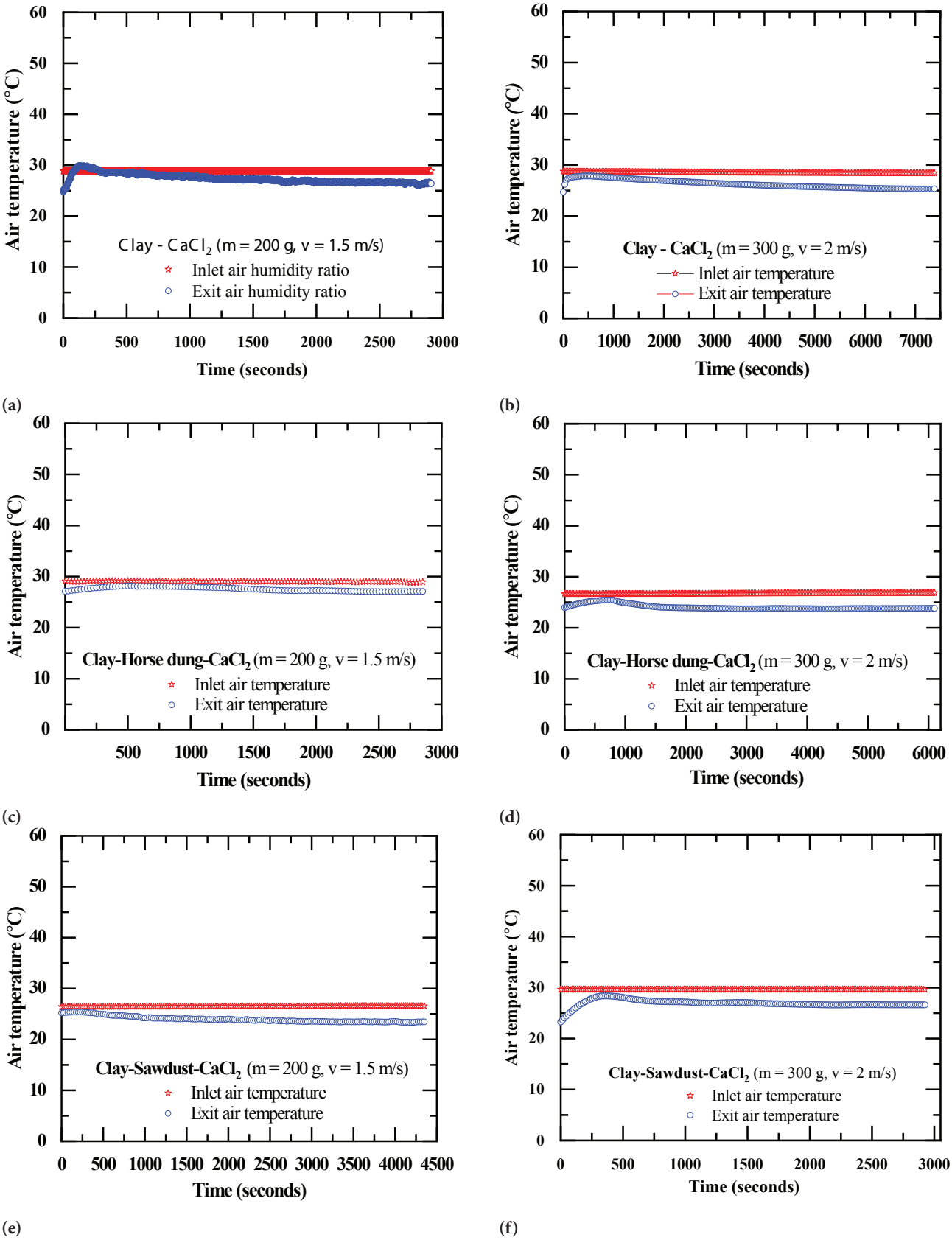

Figure 7. Air temperature characteristics of different desiccants for adsorption process.

of 28.74°C (see Figure 7(b)). For 0.0045 kg/s mass flow rate of process air, pressure drop varies from 0.34 to 0.29 m of water column. Once the process had finished, the bed mass increased by 5.84% and 3.4%, respectively, with dry desiccant bed masses of 200 g and 300 g. The transient change of the bed's exit air humidity ratio and air temperature of clay-horse dung-calcium chloride for different bed masses and air velocities is shown in Figure 6(c) - 6(d) and Figure 7(c) - 7(d). During the initial period of the process, the maximum decrease in humidity ratio for 200 g bed mass is 29.55% (see Figure 6(c)). In contrast, for 300 g, the reduction in humidity ratio is 41.89% (see Figure 6(d)). The maximum increase in temperature for 200 g bed mass is 3.42% (see Figure 7(c)), whereas for 300 g, the increase is 5.64% (see Figure 7(d)). The maximum decrease in humidity and increase in temperature is due to a higher surface area of 0.93 m^2 for 300g, whereas the available surface for 200 g bed mass is 0.62 m^2. The increased air velocity and bed surface accelerate the adsorption rate. With time, the adsorption rate decreases and steadily progresses for 200 g and 300 g bed masses. At the end, bed mass is increased by 4% and 2.93% for 200 g and 300 g bed masses at 1.5 m/s and 2 m/s inlet air velocities of bed, respectively. The transient change of the bed's exit air humidity and air temperature for 200 g and 300 g clay-sawdust-calcium chloride desiccants at the bed's inlet air velocity of 1.5 m/s, 2 m/s is shown in Figure 6(e) – 6(f) and Figure 7(e) -7(f). The humidity ratio declines to 55% of bed inlet air humidity during the early stages of the process for 200 g bed mass. It rises to a maximum of 70% of bed inlet air humidity. The bed's exit air temperature drops to a minimum of 88% of the bed's inlet air temperature and rises to a maximum of 25% of the bed's inlet air temperature. For 300 g bed mass, the humidity ratio attains a maximum drop of 57% of bed inlet air humidity. When the process is finished, the humidity reaches 67% of inlet air humidity. The bed exit air temperature air exceeds 95% of the temperature of bed intake air and reaches a minimum of 89% of air inlet temperature. The bed mass increases by 4.45% for 200 g and 2.22% for 300 g bed masses during the adsorption process, respectively.

The results in Figures 6 and 7 indicate a maximum drop in exit air humidity ratio and a maximum rise in exit air temperature within 500 s of the process. Within this period, the adsorption intensity is higher for all the clay and clay-additives-based desiccant beds. Though there is an increase in the temperature of bed exit air, it drops below the inlet air temperature. The drop in bed exit air temperature is less and remains steady compared to bed inlet air temperature. The results thus reveal the isothermal adsorption behavior of clay and clay-additives-based desiccants in fluidization.

In the adsorption process within the fluidized bed, we observed that the exit air humidity ratio is lower than the inlet air humidity ratio. This is expected as the sorbent material adsorbs moisture from the air, reducing the moisture content in the exit air. Regarding the temperature behavior, although adsorption is an exothermic process that theoretically releases heat known as the heat of adsorption, the observed decrease in the exit air temperature can be attributed to the unique dynamics of the fluidized bed. In fluidized bed systems, the constant mixing of particles and air promotes efficient heat transfer and allows the sorbent to dissipate the released heat effectively. Thus, hot spots are effectively dissipated, resulting in isothermal adsorption conditions. Additionally, the airflow in the bed has a cooling effect, which counterbalances the heat released during adsorption, resulting in a lower exit air temperature.

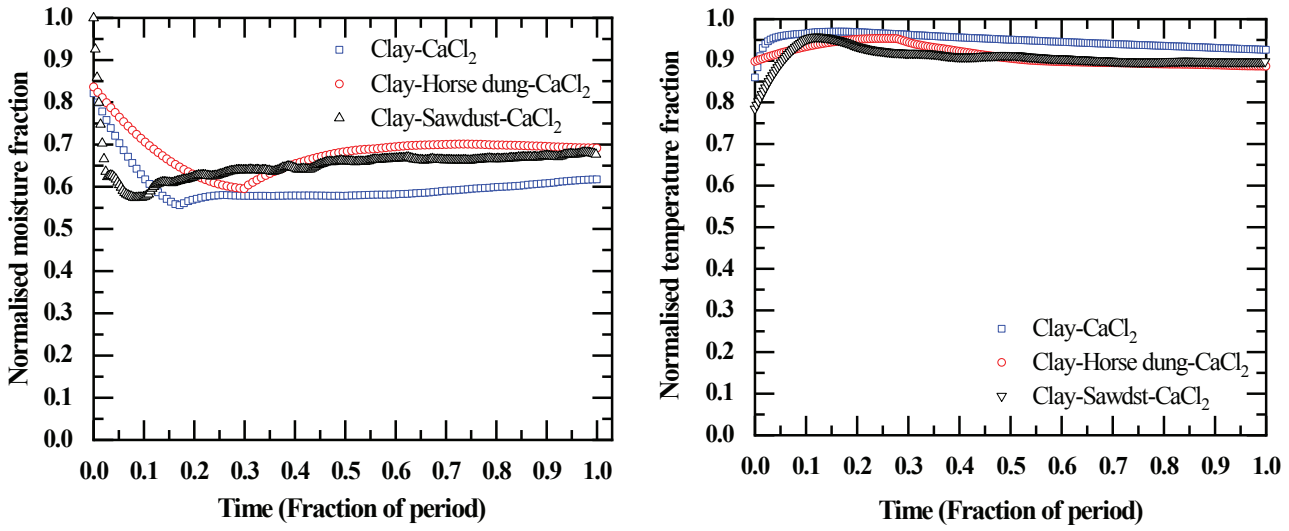

(a) (b)

Figure 8. Normalized (a) humidity ratio and (b) temperature fraction of process air for different fluidized beds at m = 300 g, v = 2 m/s.

Thus, the observed reduction in exit humidity and exit temperature can be explained by the combined effects of adsorption and the cooling influence of the airflow within the fluidized bed, leading to effective moisture removal with moderate temperature control. Apart from hot spot dissipation and cooling effect, lower residence time for air in bed and higher heat capacities [see Table 1] of clay and clay-additives-based composite desiccants control the increase in bed exit air temperature concerning inlet air temperature in fluidization.

Performance comparison of clay and clay-based calcium chloride adsorbents in vertical fluidized beds for dehumidification

The comparison of clay-additives-calcium chloride composite desiccants water vapor and process air temperature is shown in Figures 8 (a) and (b). It is reported that the normalized humidity ratio for clay-calcium chloride is 0.56, clay-sawdust-calcium chloride is 0.57 and clay-horse dung-calcium chloride fluidized desiccant beds is 0.60 (see Figure 8(a)). Clay-calcium chloride desiccants with the lowest value of humidity ratio exhibit a higher rate of adsorption than clay-additives-calcium chloride desiccants. The higher adsorptivity is due to higher dryness due to lower initial bed water content. Clay-based desiccants have a higher density than additives-based ones, resulting in higher residence and contact time for process air and higher heat and mass transfer rates. Composite desiccants made with clay additions have less absorptivity due to the shorter contact duration. The higher porosity of clay-additives-based adsorbents reduces the thermal conductivity and diffusivity of adsorbents, reducing the heat transfer rate in the clay-additives-based fluidized beds [40, 41]. Even though clay-based desiccants have low porosity, they have a higher adsorption rate because of their more considerable pore volume and higher interfacial area of interconnected macro-pores, as observed in Figure 2. With time, the absorptivity of the clay-calcium chloride adsorbent bed is higher than the absorptivity of the clay-additives-based composite desiccant bed [see Figure 8(a)]. Adsorption heat released with increased adsorption rate increases the bed outlet air temperature. The maximum value of normalized temperature is 0.97 for clay-based desiccants compared to clay-additives-based composite desiccants (see Figure 8 (b)). For all fluidized beds, the point of maximum temperature coincides with the point of the lower humidity value. The maximum temperature attained by the outlet air for clay-calcium chloride, clay-horse dung-calcium chloride and clay-sawdust-calcium chloride beds are 27.84°C, 25.42°C and 28.37°C respectively. The lower exit temperature of the adsorbed air stream may be attributed to using inert materials like clay, horse dung and sawdust in desiccant preparation [22, 42]. Applying additives of horse dung and sawdust with natural clay increases heat capacity and simultaneously decreases the thermal conductivity and thermal diffusivity of clay-additive desiccants (see Table 1).

Compared to clay desiccants, the thermo-physical properties of additives-based composite desiccants lessen the dissipation of adsorption heat to fluidized air. For clay-additive desiccants, the bed water uptake capacity immediately falls from the point of higher absorptivity forward, whereas, for clay beds, the absorptivity progressively declines. Once the process has finished, the bed water amount is increased by 3.4% for clay-calcium chloride, 2.93% for clay-horse dung-calcium chloride and 2.22% for clay-sawdust-calcium chloride beds.

The lower adsorptive nature of low-density clay-additives-based calcium chloride desiccants is due to reduced residence time for air in fluidization. Low-density adsorbents may experience uneven fluidization, which causes channeling and bypassing, where air flows through preferential paths, further reducing the effective active interfacial mass transfer area with the desiccants and thus limiting the adsorption of water vapor.

In the case of clay-horse dung-calcium chloride and clay-sawdust-calcium chloride composites, the adsorbed water vapor may form a layer on the surface of the desiccants in less time as compared to heavier clay-calcium chloride desiccants. The water vapor layer over the desiccant particles minimizes the available surface area for water vapor adsorption. Since adsorption is a surface-driven process, any reduction in the effective surface area significantly lowers the desiccant's performance.

The linear variation of porosity along the fluidized bed height is shown in Figure 9(a). The minimum and maximum bed lengths in fluidization with bed mass of 300 g and velocity of air at 2 m/s are 150 and 250 mm, 210 and 450 mm, 250 and 650 mm for clay-calcium chloride, clay-horse dung-calcium chloride and clay-sawdust-calcium chloride desiccant beds. The estimated minimum and maximum porosity distribution values are 0.56 and 0.72, 0.50 and 0.76, 0.45 and 0.78 for clay-calcium chloride, clay-horse dung-calcium chloride and clay-sawdust-calcium chloride desiccant beds. For identical bed masses of 300 g, additive-based desiccant has lower density and higher bed heights than clay-based fluidized desiccant beds. The axial porosity distribution reveals more adsorption sites in clay-additives-based beds than higher active adsorption sites in clay-based desiccant beds. The higher intensity of fluidization and a greater number of active adsorption sites (see Figure 2(a)) results in higher absorptivity as indicated by higher total adsorption capacity for clay-calcium chloride fluidized bed. Apart from fluidization, the higher clay content and inter-particle macro-pores [see Figure 2] in clay-calcium chloride desiccants result in higher water uptake and increased adsorption rate [43]. As shown in Figure 9(b), the calculated total adsorption quantities for identical 300 g bed mass are 30.09 g, 21.84 g and 27.02 g for clay-calcium chloride, clay-horse dung-calcium chloride and clay-sawdust-calcium chloride fluidized adsorbent beds. Due to more pores with a higher quantity of calcium

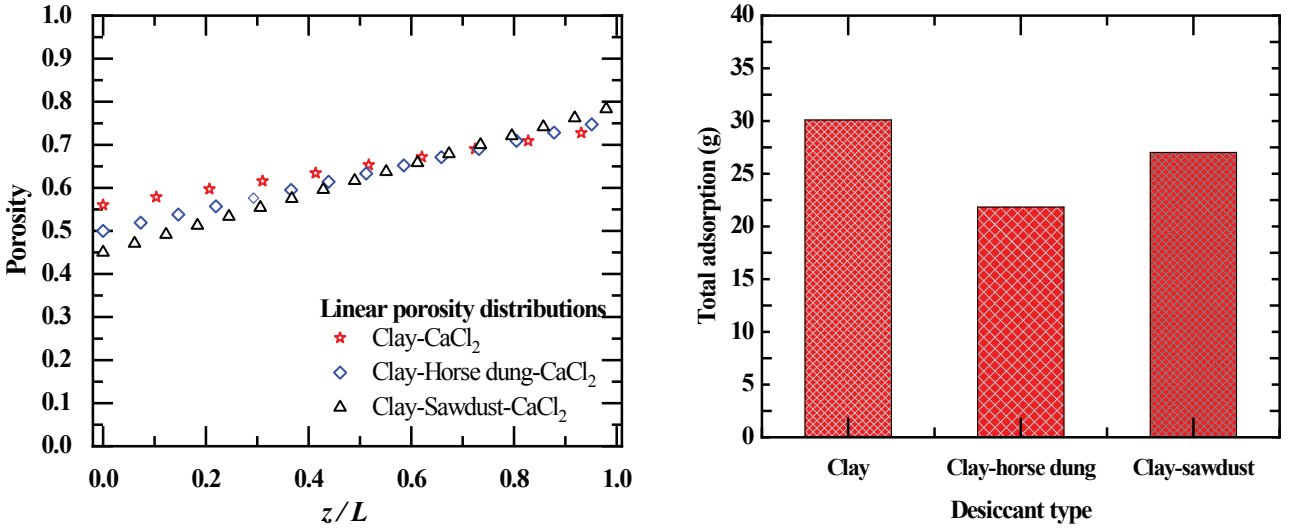

(a) (b)

Figure 9. (a) Porosity variation along the bed length and (**b**) Total adsorption rate for identical mass of fluidized beds at m = 300 g, v = 2 m/s.

chloride impregnated, the clay-calcium chloride fluidized bed has a higher overall adsorption capacity.

Sensible heat factor and Exergy efficiency

The sensible and latent heat loads are calculated for the weights of desiccant beds, which are calculated for 200 g and 300 g, and the values are tabulated in Table 3. For all the cases, the results reveal that the average latent heat load decrease is higher than the sensible heat load increase. Hence, the overall heat load of the cooling system will decrease. It is observed that total heat load reduction is higher for clay-calcium chloride than for clay-additives-calcium chloride composite desiccants. Higher heat load reduction is due to higher moisture uptake, as Figure 9(b) indicates. Due to lower moisture uptake in clay-additive-calcium chloride beds, the heat load reduction is lesser, as shown in Table 4.

The sensible heat factor, which is a function of total heat load, is considered when designing the air conditioning process. Figure 10 shows the sensible heat factor for clay and clay-additives-based calcium chloride composite desiccant for different bed masses and bed inlet air velocities. For the identical bed masses of 200 g, the decrease in sensible heat and latent heat loads are 21% and 79% for clay-calcium chloride bed, 29% and 71% for clay-horse dung bed and 34% and 66% for clay-saw dust-calcium chloride beds, respectively. With the increase in bed mass and air velocity, the sensible heat factors increase due to the availability of more bed surface area for dehumidification of process air. The result shows that the decrease in latent heat load is higher for clay-calcium chloride beds as compared to clay-additives-calcium chloride beds, whereas a reduction of sensible heat load is higher for clay-additives-calcium chloride beds. The higher decrease in sensible heat load in additive-based desiccants is attributed to the higher heat capacity of composite desiccants. The higher heat capacity, initial water content and lower thermal conductivity (see Table 1) of additive-based desiccants decrease the sensible heat load. The results indicate an average sensible heat

Table 4. Total heat load reduction by clay and clay-additives based composite desiccants

Type of desiccant	Weight of bed (m), g	Sensible heat (Q_S), J/kg	Latent heat (Q_L), J/kg	Net decrease in total heat load (Q_L-Q_S), J/kg
Clay-calcium chloride	200	1631.92	5074.75	3442.83
	300	1912.19	5510.35	3598.16
Clay-horse dung-calcium chloride	200	858.32	1866.23	1007.91
	300	2563.67	3943.62	1379.95
Clay-sawdust-calcium chloride	200	2435.02	4170.79	1735.77
	300	2527.94	4271.75	1743.81

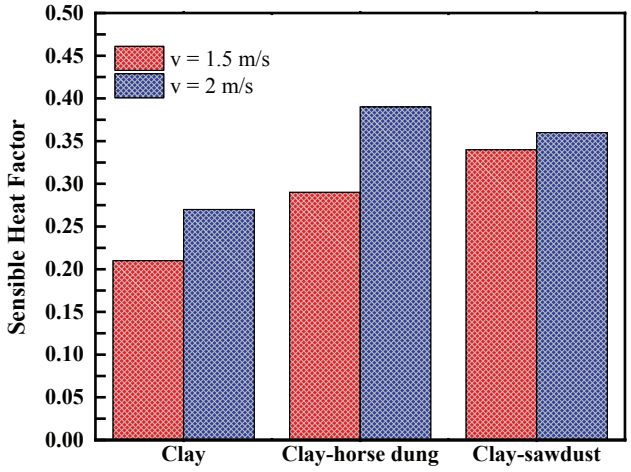

Figure 10. Sensible heat factor for different fluidized beds in dehumidification.

factor of 0.30 for clay and clay-additives-based dehumidification systems. The portion of the latent heat load handled by these dehumidification systems is 70 % compared to a sensible heat load of 30% [Table 5]. The results show the potential of clay and clay-additives-based desiccants in providing thermal comfort in hot and humid climates for sorption-based air conditioning systems.

The variation of exergy efficiency with time for different bed masses and air velocity are shown in Figure 11. The difference in exergy efficiency during dehumidification process by the fluidized clay and clay-additives based calcium chloride composite desiccants are seen in Figure.11. The estimated average rate of total exergy at bed inlet and exit are 369.4-191 kJ/s, 327-163 kJ/s and 638.3 - 264 kJ/s for 200 g clay-calcium chloride, clay-horse dung calcium chloride and clay-sawdust-calcium chloride desiccant beds. While for 300 g bed mass, the average exergy values at desiccant bed inlet and exit are 273.49 -107.04kJ/s, 612.23-213.38 kJ/s and 433.36-120.52kJ/s respectively. From Figures 11 (a) and (b) it is clear that, the rate of exergy efficiency was higher in the initial period of dehumidification process. It reaches its peak value between 500 s to 1000 s of process time and after that the exergy efficiency decreases and reaches its minimum value. The peak value is reached up to the point of release of heat of adsorption. The released heat due to adsorption of moisture increases the exergy losses which lowers the exergy efficiency. From Figure.11 (b) it is observed that point of peak value of efficiency for clay-calcium chloride bed leads the peak point for clay-horse dung-calcium chloride bed followed by clay-saw dust-calcium chloride bed. The delayed attainment of peak value for clay based composite desiccant is attributed due to micro-pore volume, higher density, lower porosity and higher dryness (See Table 1).

The attainment of higher exergy efficiency in clay-based desiccants is due to lower pressure drop through the bed. The lower pressure drop minimizes the work input to the system. The pressure drop through the bed of clay-calcium chloride is 372.78 Pa, whereas for clay-horse dung-calcium chloride, it is 539.55 Pa, and for clay-walled dust-calcium chloride, the bed is 1226.25 Pa. The lower exergy efficiency values for clay-additives-based composite desiccant beds reveal the slower adsorptive nature compared to clay-based composite desiccant beds. The higher latent heat load controlled by clay-calcium chloride composite desiccants increases the exergy efficiency of process air exiting the bed. The results reveal that a higher decrease in latent heat increases exergy efficiency. In contrast, a higher reduction

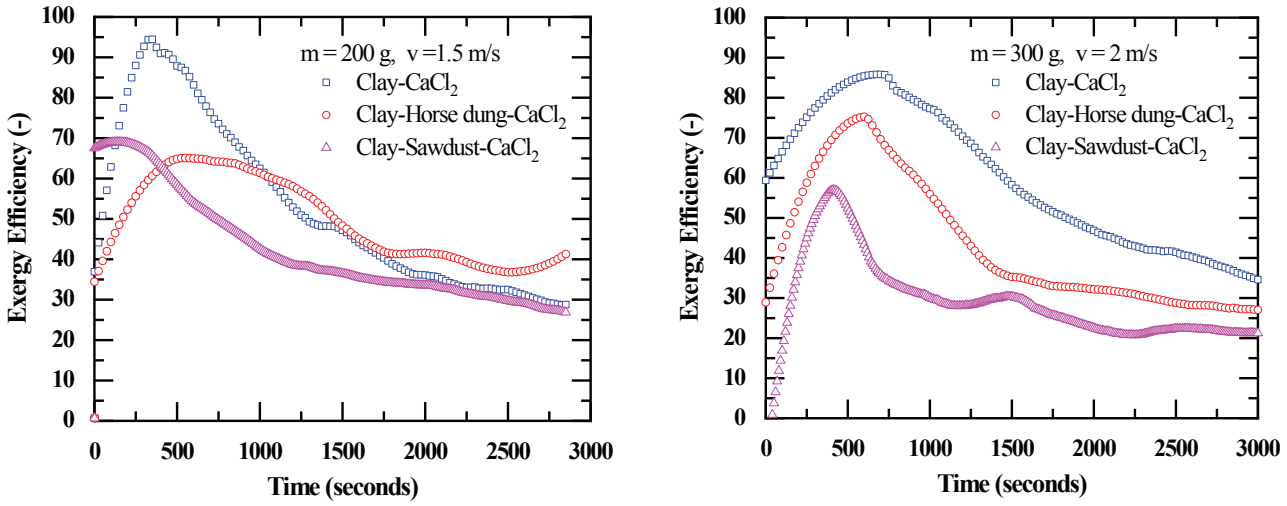

Figure 11. Transient variation of exergy efficiency for fluidized clay and clay-additives composite desiccants in dehumidification.

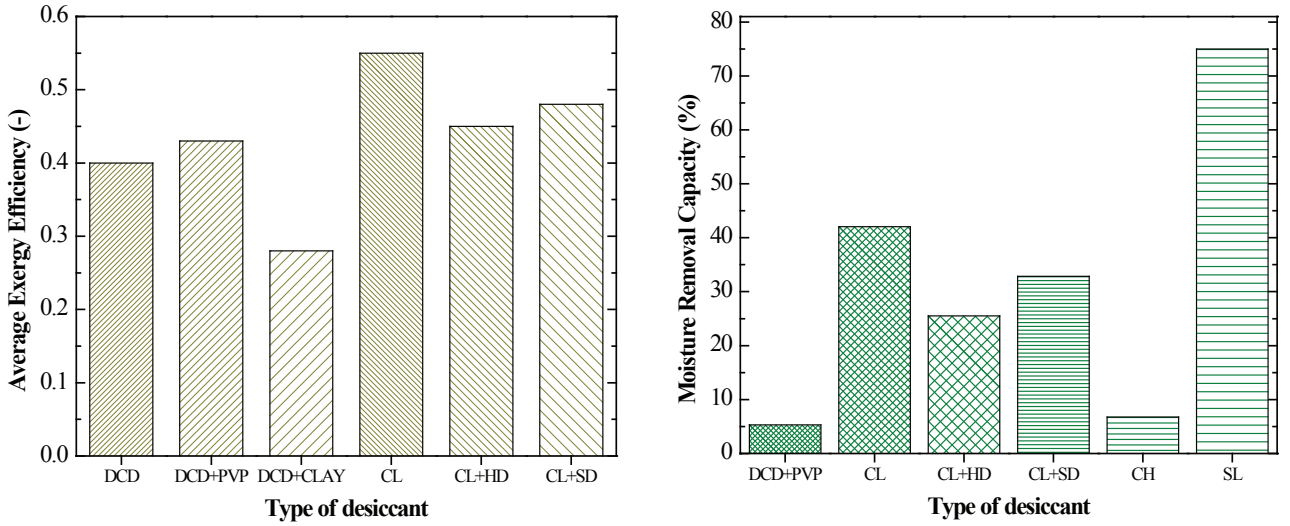

(a) (b)

Figure 12. Assessment of (a) exergy efficiency and (b) moisture removal capacity for different dehumidification systems

in sensible heat lowers the exergy efficiency in clay additives-based composite desiccant beds.

The average exergy efficiency of the present work clay-calcium chloride (CL), clay-horse dung-calcium chloride (CL+HD) and clay-sawdust-calcium chloride (CL+SD) are plotted in Figure 12(a) and are compared with the literature results. The moisture removal capacity is calculated by knowing the bed inlet and exit air humidity ratio and is plotted in Figure 12(b). The average exergy efficiencies for the dried cow dung (DCD), cow dung combined with polyvinyl pyrrolidone (DCD+PVP), and dried cow dung with clay (DCD+ClAY) dehumidification systems are 0.40, 0.43, and 0.35, respectively. Notably, the exergy efficiency of the DCD+PVP system is 1.8% and 3.6% higher than that of the DCD and DCD+clay systems. Correspondingly, the moisture removal capacity of DCD+PVP dehumidification systems is 5.3 % and 18.37% greater than DCD and DCD+clay systems [27]. Higher moisture removal capacity in the clay-calcium chloride dehumidification system means higher exergy efficiency presented in Figure 12(a). The results reveal lower exergy efficiency in the clay-additives-calcium chloride dehumidification system than in the clay-calcium chloride system. Lesser exergy efficiency is attributed to lesser moisture removal capacity, as presented in Figure 12(b). The moisture removal capacity of present work dehumidification systems is compared with DCD+PVP, clay-calcium chloride (CH) [39] and silica gel (SL) [44] dehumidification systems available in literature. Silica gel dehumidification system has a higher % moisture removal capacity of 75% compared to clay and clay-additives-based calcium chloride composite desiccants. However, silica gel exhibits higher dehumidification capacity but significantly increases the air temperature. Clay-based dehumidification systems offer advantages with respect to moisture removal and temperature control.

Besides dehumidification, the advantage of clay-based desiccants is the lower temperature of the air that leaves the desiccant bed. The process air leaves the clay-based composite desiccants at much lower temperatures than the silica gel desiccant bed. The average drop in temperature of clay and clay-additives composite desiccant bed exit air concerning inlet air temperature is 0.80°C (fluidized bed) and 1.80 °C (packed bed) [39]. The average silica gel bed exit air temperature increase is 17.10°C concerning inlet air temperatures [44]. Lower temperatures prevailing in clay and clay-additives composite desiccant systems as compared to silica gel will promote cooling energy saving in sorption-based systems.

CONCLUSION

In this work, an experimental study was conducted to understand the adsorption characteristics of a new composite desiccant prepared from natural materials. Utilization of naturally available clay and biomaterials such as horse dung and sawdust, which are considered as wastes added value in the preparation of clay-based composite desiccants. Horse dung traditionally employed in the pot making finds relevance in desiccant preparation. The following conclusions can be drawn from the experimental study on transient adsorption characteristics of atmospheric water vapor with clay and clay-additives based calcium chloride composite desiccants in vertical fluidized bed:

1. The scanning electron microscope micrographs reveal the presence of interparticle macro-pores and higher mass of calcium chloride in clay-calcium chloride adsorbents.

2. The fluidization of higher porosity and low-density desiccants decreases the mass transfer area involved in adsorption. For the set period of the process, the lower active interfacial area may lead to a slower adsorptive nature of clay-additives-calcium chloride desiccants compared to clay-calcium chloride adsorbents in fluidization.
3. The linear porosity distribution in fluidization demonstrates higher total adsorption capacity for clay-based desiccants, which is 38% and 12 % higher than that of clay-horse dung- calcium chloride and clay-sawdust-calcium chloride desiccant dehumidification systems.
4. Clay-calcium chloride vertical fluidized bed dehumidification system achieves higher total heat load reduction of 62% and 52% as compared to clay-horse dung-calcium chloride and clay-sawdust-calcium chloride desiccant dehumidification systems. As a result the overall heat load of the cooling system will significantly decrease.
5. The exergy efficiency analysis reveals that the clay- calcium chloride fluidization dehumidification system has a better exergy efficiency of 55% as compared to 45% for clay-additives-calcium chloride composite desiccants.
6. Using waste material like horse dung and sawdust with clay in desiccant preparation leads to a new family of desiccants making the technology more eco-friendly and helping promote sustainable goal development.

NOMENCLATURE

Symbol Meaning

A_1	Cross sectional area of pipe (m^2)
A_2	Cross sectional area of orifice meter (m^2)
C_p	Specific heat (J/kg K)
C_d	Coefficient of discharge of orifice (-)
d	Diameter (m)
E_X	Exergy (J)
E_Y	Exergy destruction (J)
g	Acceleration due to gravity (m/s^2)
h	Manometer deflection (m)
h_{fg}	Latent heat of vapor (J/kg)
L	Length of bed (m)
m	Mass flow rate (kg/s)
m	Weight of desiccant bed (g)
M	Total adsorption rate (g/s)
P	Pressure (N/m^2)
Q_{act}	Actual volume flow rate (m^3/s)
Q_S	Sensible heat load (J/kg)
Q_L	Latent heat load (J/kg)
R	Gas constant (J/kg K)
H_R	Humidity ratio of air (kg/kg of dry air)
t	Time (s)
T	Temperature (°C)
v	Superficial velocity (m/s)
x	Manometer deflection (m)
z	Step length of the bed (m)

Greek symbols

ε	Porosity (-)
ρ	Density (kg/m^3)
η	Exergy efficiency (-)
ϕ	Relative Humidity (-)
ω	Overall uncertainty (-)
∂	Differential operator (-)
Δ	Small change (-)

Subscripts

a	Process air
ads	Adsorption
b	Bed
e	Exit
sat	Saturation
min	Minimum
max	Maximum
mf	Minimum fluidization
i	Inlet
o	Ambient
w	Vapor

Abbreviations

$CaCl_2$	Calcium chloride
GI	Galvanized iron
HCl	Hydro chloride
RH	Relative humidity
SEM	Scanning electron microscope
SHF	Sensible heat factor
VFD	Vertical fluidized bed

ACKNOWLEDGEMENT

The authors acknowledge the administrative and technical support provided by V. P. Dr. P. G. Halakatti College of Engineering and Technology Vijayapur-586103, Karnataka state, India, to carry out this research study.

CONFLICTS OF INTEREST

The authors declare no conflict of interest.

CREDIT AUTHORSHIP CONTRIBUTION STATEMENT

C R Hiremath: Conceptualization, Investigation, Methodology, Writing - original draft. **Ravikiran Kadoli:** Supervision, Writing - review and editing. **R J Talapati:** Writing - review and editing

REFERENCES

[1] Zhang Y, Wang W, Zheng X, Cai J. Recent progress on composite desiccants for adsorption-based dehumidification. Energy 2024;302:131824. [CrossRef]

[2] Kaushik SC, Verma A, Tyagi SK. Advances in solar absorption cooling systems: an overview. J Therm Eng 2024;10:1044-1067. [CrossRef]

[3] Sharafian A, Bahrami M. Assessment of adsorber bed designs in waste-heat driven adsorption cooling systems for vehicle air conditioning and refrigeration. Renew Sustain Energy Rev 2014;30:440-451. [CrossRef]
[4] Subramanyam N, Maiya MP, Murthy SS. Application of desiccant wheel to control humidity in air-conditioning systems. Appl Therm Eng 2004;24:2777-2788. [CrossRef]
[5] Enteria N, Mizutani K. The role of the thermally activated desiccant cooling technologies in the issue of energy and environment. Renew Sustain Energy Rev 2011;15:2095-2122. [CrossRef]
[6] Hiremath CR, Ravikiran K. Experimental analysis of low-temperature grain drying performance of vertical packed clay and clay-additives composite desiccant beds. Sadhana 2021;46:1-6. [CrossRef]
[7] Ji JG, Wang RZ, Li LX. New composite adsorbent for solar-driven fresh water production from the atmosphere. Desalination 2007;212:176-182. [CrossRef]
[8] Lv B, Zhao Z, Deng X, Fang C, Xing B, Dong B. Hydrodynamics and adsorption performance of liquid-solid fluidized bed with granular activated carbon for removal of copper ions from wastewater. J Clean Prod 2021;328:129627. [CrossRef]
[9] Krzywanski J, Grabowska K, Sosnowski M, Zylka A, Kulakowska A, Czakiert T, et al. Heat transfer in adsorption chillers with fluidized beds of silica gel, zeolite, and carbon nanotubes. Heat Transf Eng 2021;43:172-182. [CrossRef]
[10] Hamed AM. Experimental investigation on the adsorption/desorption processes using solid desiccant in an inclined-fluidized bed. Renew Energy 2005;30:1913-1921. [CrossRef]
[11] Horibe A, Husain S, Inaba H, Haruki N, Tu P. An experimental investigation of sorption process in fluidized bed with cooling pipe. J Heat Transf 2008;130:114509. [CrossRef]
[12] Ye J, Luo Q, Li X, Xu Q, Li Z. Sorption drying of soybean seeds with silica gel in a fluidized bed dryer. Int J Food Eng 2008;4. [CrossRef]
[13] Sobrino C, Almendros-Ibáñez JA, Santana D, De Vega M. Fluidization of Group B particles with a rotating distributor. Powder Technol 2008;181:273-280. [CrossRef]
[14] Hamed AM, Abd El Rahman WR, El-Emam SH. Experimental study of the transient adsorption/desorption characteristics of silica gel particles in fluidized bed. Energy 2010;35:2468-2483. [CrossRef]
[15] Wang Q, Gao X, Xu JY, Maiga AS, Chen GM. Experimental investigation on a fluidized-bed adsorber/desorber for the adsorption refrigeration system. Int J Refrig 2012;35:694-700. [CrossRef]
[16] Horibe A, Haruki N, Hiraishi D. Continuous sorption and desorption of organic sorbent powder in two connected fluidized beds. J Therm Sci Technol 2012;7:563-576. [CrossRef]
[17] Zettl B, Englmair G, Somitsch W. An open sorption heat storage concept and materials for building heat supply. Energy Procedia 2015;73:297-304. [CrossRef]
[18] Li X, Wang L, Jia L, Cai W. Numerical and experimental study of a novel compact micro fluidized beds reactor for CO_2 capture in HVAC. Energy Build 2017;135:128-136. [CrossRef]
[19] Chairunnisa, Yu H, Saren S, Miksik F, Conte P, Miyazaki T, et al. A review of recent advances in sustainable preparation of high-performing activated carbon for dehumidification technology. J Mater Sci 2024;59:1-36. [CrossRef]
[20] Mittal H, Al Alili A, Alhassan SM. Development of high efficacy super-porous hydrogel composites-based polymer desiccants to capture water vapors from moist air. Adsorption 2024;30:841-857. [CrossRef]
[21] Kumar M, Yadav A. Composite desiccant material "$CaCl_2$/Vermiculite/Saw wood": A new material for fresh water production from atmospheric air. Appl Water Sci 2017;7:2103-2111. [CrossRef]
[22] Hiremath CR, Kadoli R, Katti VV. Experimental and theoretical study on dehumidification potential of clay-additives based calcium $CaCl_2$ desiccants. Appl Therm Eng 2018;129:70-83. [CrossRef]
[23] Liang JD, Hsu CY, Hung TC, Chiang YC, Chen SL. Geometrical parameters analysis of improved circulating inclined fluidized beds for general HVAC duct systems. Appl Energy 2018;230:784-793. [CrossRef]
[24] Timsina R, Thapa RK, Moldestad BME, Eikeland MS. Effect of particle size on flow behavior in fluidized beds. Int J Energy Prod Manag 2019;4:287-297. [CrossRef]
[25] Singh A, Kumar S, Dev R. Studies on cocopeat, sawdust and dried cow dung as desiccant for evaporative cooling system. Renew Energy 2019;142:295-303. [CrossRef]
[26] Politi D, Sidiras D. Modified spruce sawdust for sorption of hexavalent chromium in batch systems and fixed-bed columns. Molecules 2020;25:5156. [CrossRef]
[27] Dasar SR, Boche AM, Yadav AK. Sorption-desorption characteristics of dried cow dung with PVP and clay as composite desiccants: Experimental and exergetic analysis. Renew Energy 2023;202:394-404. [CrossRef]
[28] Suranjan Salins S, Reddy SK, Kumar S, Nair PS. Application of biomass-based wood shaving packing in a liquid desiccant dehumidification system - a source of sustainable energy. Int J Sustain Energy 2024;43:2287783. [CrossRef]
[29] Hiremath CR, Kadoli R. Experimental studies on heat and mass transfer in a packed bed of burnt clay impregnated with $CaCl_2$ liquid desiccant and exploring the use of gas side resistance model. Appl Therm Eng 2013;50:1299-1310. [CrossRef]

[30] Chen H, Peng YH, Wang YL. Thermodynamic analysis of hybrid cooling system integrated with waste heat reusing and peak load shifting for data center. Energy Convers Manag 2019;183:427-439. [CrossRef]
[31] Hiremath CR, Katti VV, Kadoli R. Experimental determination of specific heat and thermal conductivity of clay+additives-$CaCl_2$ composite desiccant. Procedia Mater Sci 2014;5:188-197. [CrossRef]
[32] Wu SY, Baeyens J. Effect of operating temperature on minimum fluidization velocity. Powder Technol 1991;67:217-220. [CrossRef]
[33] Rachayya HC. Studies on dehumidification potential of clay with additives and impregnated with $CaCl_2$ composite desiccants [dissertation]. Surathkal (IN): National Institute of Technology Karnataka; 2019.
[34] Ramzy A, Kadoli R. Modified PGC model and its validation by experiments for heat and moisture transfer analysis in a vertical fluidized desiccant bed. Appl Therm Eng 2015;81:83-91. [CrossRef]
[35] Liang JD, Hsu CY, Hung TC, Chiang YC, Chen SL. Geometrical parameters analysis of improved circulating inclined fluidized beds for general HVAC duct systems. Appl Energy 2018;230:784-793. [CrossRef]
[36] Sarker MSH, Ibrahim MN, Aziz NA, Punan MS. Energy and exergy analysis of industrial fluidized bed drying of paddy. Energy 2015;84:131-138. [CrossRef]
[37] Kumar R, Mishra DR, Dumka P. Improving solar still performance: A comparative analysis of conventional and honeycomb pad augmented solar stills. Solar Energy 2024;270:112408. [CrossRef]
[38] Moffat RJ. Describing the uncertainties in experimental results. Exp Therm Fluid Sci 1988;1:3-17. [CrossRef]
[39] Hamed AM. Theoretical and experimental study on the transient adsorption characteristics of a vertical packed porous bed. Renew Energy 2002;27:525-541. [CrossRef]
[40] Demir H, Mobedi M, Ülkü S. Effects of porosity on heat and mass transfer in a granular adsorbent bed. Int Commun Heat Mass Transf 2009;36:372-377. [CrossRef]
[41] Zheng X, Wang LW, Wang RZ, Ge TS, Ishugah TF. Thermal conductivity, pore structure and adsorption performance of compact composite silica gel. Int J Heat Mass Transf 2014;68:435-443. [CrossRef]
[42] Majumdar P, Sarwar MK. Performance of a desiccant dehumidifier bed with mixed inert and desiccant materials. Energy 1994;19:103-116. [CrossRef]
[43] Wang T, Tian S, Li G, Sheng M, Ren W, Liu Q, et al. Experimental study of water vapor adsorption behaviors on shale. Fuel 2019;248:168-177. [CrossRef]
[44] Pesaran AA, Mills AF. Moisture transport in silica gel packed beds-II. Experimental study. Int J Heat Mass Transf 1987;30:1051-1060. [CrossRef]